Comparative Study of Turbulence Models in Predicting Turbulent Pipe Flow Part II: Reynolds Stress and k-ϵ Models

A. Pollard* and R. Martinuzzi†
Queen's University, Kingston, Ontario, Canada

Developing turbulent pipe flow in a smooth circular pipe with a length of about 80 diameters is simulated at Reynolds numbers of 10,000, 38,000, 90,000, and 380,000, using seven different turbulence models. The governing equations are solved in their fully elliptic forms. The predictions for the velocity, turbulence kinetic energy, dissipation rate, and Reynolds stress fields are compared to available experimental data, and the relative performance of the models is assessed. This paper is Part II of a two-part study in which a total of eleven turbulence models are compared. In Part I, two k-ϵ models and four algebraic stress models were compared. Here, the k-ϵ models and five Reynolds stress models are considered. It has been found that the results obtained with a low Reynolds number k-ϵ model are in better agreement with the experimental data than those obtained using other models.

Nomenclature

B,C = constants in turbulence models
D = pipe diameter
f,F = functions in turbulence models
k = turbulence kinetic energy
P = production term for k
P^* = mean hydrostatic pressure
P^{ij} = production of Reynolds stresses
p = pressure fluctuation
Re = Reynolds number, $\equiv U_{avg}D/\nu$
R_k = turbulence Reynolds number, $\equiv k^{1/2}x_n/\nu$
R_t = turbulence Reynolds number, $\equiv k^2/\epsilon\nu$
T^{ij} = transport term for Reynolds stresses
U,V = axial and radial mean velocity
u_τ = friction velocity
U_{avg}, U_b = average axial mean velocity
U^+ = normalized velocity, $\equiv U/u_\tau$
$-\rho\overline{u^iu^j}$ = Reynolds stress tensor
x,r = axial, radial coordinate
x_n = Cartesian coordinate normal to a solid surface
y^+ = normalized wall coordinate, $\equiv yu_\tau/\nu$
γ = constant in pressure-strain model
δ = height normal to surface of grid point directly adjacent to wall
δ_ν = local height of viscous sublayer
δ^+ = $\equiv \delta_\nu u_\tau/\nu$
ϵ = homogeneous dissipation rate of k
ϵ^{ij} = dissipation rate of $\overline{u^iu^j}$
κ = von Kármán's constant
λ = friction factor, $\equiv -(4D/\rho U_{avg}^2)/(dP^*/dx)$
μ_t = turbulence "eddy" viscosity
ν = kinematic viscosity, $\equiv \mu/\rho$
ρ = density
σ_k,σ_ϵ = turbulence Prandtl-Schmidt numbers
τ_w = wall shear stress
τ^{ij} = shear stress tensor
Φ^{ij} = pressure-strain term
Ψ,ψ = general variables (scalar or vector)

Received Dec. 10, 1987; revision received Jan. 16, 1989.

*Associate Professor, Department Mechanical Engineering.
†Student, Department Mechanical Engineering, currently at Lehrstuhl für Strömungsmechanik, Universität Erlangen-Nürnberg, FRG.

Introduction

THIS paper represents the second part of a performance study of eleven models of turbulence. The flow situation considered is developing turbulent flow in a pipe. In Part I of this study,[1] two k-ϵ models and four algebraic stress models (ASM) were used. Here, attention is concentrated on comparing the same two k-ϵ models and five Reynolds stress closure (RSM) models. As explained in Part I, the rationale for the study is to see how well various models of turbulence perform under controlled conditions of standardized computer coding, discretization schemes, pressure velocity coupling, equation solvers, boundary condition implementation, initial conditions, and grid distributions.

The k-ϵ model variants used were the high Reynolds number version (see Launder and Spalding[2]), which utilizes wall functions, and a version that incorporates low Reynolds number effects (making the prescription for near-wall behavior unnecessary) developed by Lam and Bremhorst.[3] It has been shown[1] that, overall, the low Reynolds number k-ϵ model provides the best simulation of developing turbulent pipe flow but that it has limited applicability. The different ASM's were found to perform less well for low Reynolds number flow simulations; but these models provide good predictions at higher Reynolds numbers and are more versatile than the models of the k-ϵ family. In addition, the CPU times for the ASM and the k-ϵ family were found to be comparable.

The RSM models used in the present investigation effect mathematical closure by modeling terms directly within the transport equations for the velocity correlations, according to the analysis of Chou[4] for the pressure-strain and triple velocity (turbulence diffusion) terms. A precursor to these models was that of Hanjalic and Launder,[5] which provided a mechanism to account for low Reynolds number effects present in the proximity of a wall; however, it met with only modest success in predicting boundary-layer flow. A version different from Ref. 5 was proposed by Launder, Reece, and Rodi,[6] hereafter referred to as LRR75, in which attempts at making the model valid through the viscous sublayer were abandoned and expressions were developed for the wall effect term in the pressure-strain relation. A different RSM results by substituting the Naot, Shavit, and Wolfstein,[7] hereafter referred to as NSW70, prescriptions for the pressure-strain term. In all, four versions of this RSM, obtained by alternating the pressure-strain prescriptions and including or excluding the wall effect term, were tested. The fifth RSM used in the present analysis

was developed by Elghobashi and Prud'homme,[8] hereafter referred to as EP83. It combines the near-wall characteristics of Ref. 5 and the pressure-strain model of LRR75. In addition, the model also takes into account the effect of anisotropy on ϵ^{ij}.

In this study, tests were performed using the seven models mentioned above, for a pipe length of about 80 diameters at Reynolds numbers of 10,000, 38,000, 90,000, and 380,000. Uniform and nonuniform grids were used and the equations discretized using either the hybrid differencing scheme of Spalding[9] or the QUICKER scheme of Pollard and Siu.[10] The CTS-SIMPLE algorithm of Raithby and Schneider[11] or the SIMPLE-C algorithm of Van Doormaal and Raithby[12] was used to effect a solution to the governing equations.

In the next section, the various models are highlighted. A knowledgeable reader may wish to skip this section and refer directly to Table 1.

Models

The equations for the seven models employed in this study are presented in generalized tensor form (using Einstein's notation convention). The representation for the transport equations of the turbulence kinetic energy k, and dissipation rate ϵ are similar for all models. For an incompressible fluid, the k-transport equation is

$$\frac{Dk}{Dt} = \text{Diff}(k) + P - \epsilon \tag{1}$$

where,

$$\text{Diff}(k) = \nu(k)_{,\ell} - \tfrac{1}{2}(\overline{u^i u_i u^\ell}) - (\overline{pu^\ell/\rho})_{,\ell}$$

$$\epsilon = \nu \overline{u^{i,\ell} u_{i,\ell}}$$

$$P = -\overline{u^i u^\ell} U_{i,\ell} \tag{2}$$

The contribution of $(\overline{pu^\ell/\rho})_{,\ell}$ is traditionally neglected (see LRR75 or EP83).

The production term P is explicitly defined, so that only the dissipation rate and the fluctuation-velocity triple correlation need be modeled. The dissipation rate is approximated from a modeled transport equation, whereas the triple correlation is evaluated in the k-ϵ model by

$$-(\overline{u^i u_i u^\ell})_{,\ell} \rightarrow \left[\left(\frac{\nu_t}{\sigma_k}\right) k^{,\ell}\right]_{,\ell} \tag{3}$$

where $\sigma_k = 1$, as proposed by Harlow and Nakayama.[13] In the various RSM's, this term is modeled as

$$-(\overline{u^i u_i u^\ell})_{,\ell} \rightarrow \left[f'_\mu \left(c_s \frac{k}{\epsilon}\right) \overline{u^i u^\ell} k_{,\ell}\right]_{,i} \tag{4}$$

from the form originally proposed by Daly and Harlow,[14] where $c_s = 0.22$, as used by Yang et al.[15] (using the value $c_s = 0.25$ as used by LRR75 has no discernible effect on the calculations). The function f'_μ is unity for all models except that proposed by EP83.

The form of the ϵ equation is

$$\frac{D\epsilon}{Dt} = \text{Diff}(\epsilon) + \frac{\epsilon}{k}(c_{1\epsilon} f_1 P - c_{2\epsilon} f_2 \epsilon) + F_\epsilon \tag{5}$$

where, for the k-ϵ models,

$$\text{Diff}(\epsilon) = \left[\left(\nu + \frac{\nu_t}{\sigma_\epsilon}\right)\epsilon^{,\ell}\right]_{,\ell} \tag{6}$$

with $\sigma_\epsilon = 1.3$.[2] The function F_ϵ represents the contribution to the dissipation and production of ϵ due to small-scale motion and viscous effects. It is considered to be negligible everywhere except in the vicinity of a solid boundary. This term is neglected in all models except that of EP83.

In the RSM, the turbulence stress tensor is obtained by solving a modeled form of the transport equation,

$$\underbrace{\frac{\partial \overline{u^i u^j}}{\partial t} + U^\ell (\overline{u^i u^j})_\ell}_{\text{convection}} = \underbrace{\left\{-(\overline{u^i u^j u^\ell}) + \overbrace{(pu^i \delta^{j\ell} + pu^j \delta^{i\ell})}^{\text{Diff}^{ij}} + \nu(\overline{u^i u^j})^{,\ell}\right\}_{,\ell}}_{\text{diffusion}} \underbrace{- \overline{u^i u^\ell} U^{j,P^{ij}}_{,\ell} - \overline{u^i u^\ell} U^j{}_{,\ell}}_{\text{production}} \underbrace{- 2\nu \overbrace{u^{i,\ell} u^{j,}_{\ell}}^{\epsilon^{ij}}}_{\text{dissipation}} \underbrace{+ \frac{1}{\rho}\overbrace{(p(u^{i,j} + u^{j,i}))}^{\Phi^{ij}}}_{\text{pressure-strain}} \tag{7}$$

The diffusion term is modeled according to LRR75. The triple correlation is evaluated assuming that the pressure diffusion term is negligible and using

$$-(\overline{u^i u^j u^m}) \rightarrow c_s \left(\frac{k}{\epsilon}\right) \overline{u^\ell u^m} (\overline{u^i u^j})_{,\ell} \tag{8}$$

from Ref. 14, which is, according to LRR75, an acceptable approximation for this axisymmetric flow to the more general form proposed by Rotta,[16] namely,

$$\overline{u^i u^j u^m} \rightarrow -c'_s \left(\frac{k}{\epsilon}\right)\left\{\overline{u^i u^\ell}(\overline{u^j u^m})_{,\ell} + \overline{u^j u^\ell}(\overline{u^m u^i})_{,\ell} + \overline{u^m u^\ell}(\overline{u^i u^j})_{,\ell}\right\} \tag{9}$$

The production term P^{ij} is evaluated directly, but the dissipation term is modeled using the assumption of local flow isotropy,

$$\epsilon^{ij} \rightarrow \tfrac{2}{3}\epsilon \delta^{ij} \tag{10}$$

except in the version proposed by EP83, in which

$$\epsilon^{ij} = \epsilon\left(\tfrac{2}{3}\delta^{ij} - (1 - \delta^{ij}) f_s \frac{\overline{u^i u^j}}{k}\right) \tag{11}$$

with no i,j sum.

The pressure-strain term Φ^{ij} describes the mechanism by which interaction between the fluctuating pressure field and the fluctuating velocity field serves to redistribute the Reynolds stresses. The term is divided into a contribution due to the distortion of the Reynolds stress field Φ_1^{ij}, a contribution due to the distortion of the mean velocity field Φ_2^{ij}, and a term that arises because of the proximity of a solid boundary Φ_w^{ij}.

An explicit expression for the pressure-strain term can be obtained following Chou.[4] The term Φ_1^{ij} is approximated using Rotta's[16] proposal (see Table 1), in which the coefficient C_1 is assumed constant and, as argued in Ref. 1, set equal to 1.5, according to LRR75.

The second term, Φ_2^{ij}, which arises because of distortion of the mean field, is modeled differently by NSW70 and LRR75. The latter group proposes a linear combination of Reynolds stresses, which satisfies the physical and kinematic constraints proposed by Rotta[16]; for the final form, see Table 1.

The local effect of a rigid solid wall on a fluid is expressed through Φ_w^{ij}. LRR75 shows that this term, a surface integral, can be recast as a volume integral of a form similar to that of $(\Phi_1^{ij} + \Phi_2^{ij})$, which consequently leads LRR75 to model this term as

$$\Phi_w^{ij} = \left\{c_3\left(\frac{\epsilon}{k}\right)\left(\overline{u^i u^j} - \tfrac{2}{3}k\delta^{ij}\right) + c_4(P^{ij} - D^{ij})\right\} k^{3/2}/\epsilon x_n \tag{12}$$

where x_n is the distance normal to the wall.

EP83 proposes that the only significant contribution is that due to the mean field distortion, yielding

$$\Phi_w^{ij} = c_3(P^{ij} - D^{ij}) \exp(-c_4 R_k) \tag{13}$$

The values for c_3 and c_4 are obtained from a consensus (see LRR75 or Martinuzzi[17]) for near-wall values: $(\overline{u^2}/k) - (\frac{2}{3}) \approx 0.51$, $(\overline{v^2}/k) - (\frac{2}{3}) \approx -0.42$, and $(\overline{w^2}/k) - (\frac{2}{3}) \approx -0.09$, with the wall effect being neglected for the $\overline{w^2}$ equation, as in EP83.

In total, seven models can be constructed: two k-ϵ models and five RSM's, by employing the various model proposals outlined. A summary of these models is given in Table 1.

Numerical Procedure and Boundary Conditions

The reader is referred to Part I of this paper[1] to obtain an overview of the numerical procedure.

The boundary conditions used are the same for all simulations. The reader is referred to Ref. 1 for those boundary conditions not explicitly stated here.

A uniform inlet velocity field is assumed. The normal stress components of the Reynolds stress tensor $-\rho\overline{u^i u^j}$ are given the values of Champagne et al.[18] for homogeneous flow, i.e., $\overline{u^2}/k = 1.0$, $\overline{v^2}/k = 0.5$, and $\overline{w^2}/k = 0.5$; note that $-\rho\overline{uv} = 0$.

The wall boundary condition for the Reynolds shear stresses is obtained in the following manner. The pressure gradient normal to the wall is considered to be negligible throughout the control volume. A log-law velocity distribution is then assumed to exist, with only gradients perpendicular to the wall taken to be non-negligible. By integrating the now reduced near-wall U-momentum equation and making use of the continuity equation, we obtain

$$\frac{\overline{uv}}{u_\tau^2} = \frac{1}{1+\xi-(1/\kappa x_n)} - 2\xi\left(-\frac{R}{2\rho U^2}\frac{dP^*}{dx}\right) \tag{14}$$

where $\xi = \delta/R$. For the other stress components, the procedure outlined by Patel et al.[19] (see also Ref. 1) is followed.

For the low Reynolds number k-ϵ model and EP83 RSM, which are applicable even in the viscous sublayer, the physical boundary conditions for k and ϵ are directly implemented, namely,

$$\Psi_{\text{wall}} = \frac{\partial \Psi}{\partial x_n}\Big|_{\text{wall}} = 0 \tag{15}$$

Table 1 Summary of turbulence models

M	Name	$\rho\overline{uv}$	Diff(Ψ)	Φ_w^{ij}	Φ_2^{ij}
1	High Reynolds no. k-ϵ	$\frac{2}{3}\rho k\delta^{ij} - \mu_t(U^i{}_{,j} + U^j{}_{,i})$	$\left[\left(\nu + \frac{\nu_t}{\sigma_\Psi}\right)\Psi_{,\ell}\right]_{,\ell}$	N/A	N/A
2	Low Reynolds no. k-ϵ	$\mu_t = \rho C_\mu f_\mu \frac{k^2}{\epsilon}$	$\sigma_k = 1$ $\sigma_\epsilon = 1.3$	N/A	N/A
3	Naot et al., no wall term	$F_\epsilon = 0$	$\left(\nu\Psi_{,\ell} + \left[c_\Psi f'_\mu\left(\frac{k}{\epsilon}\right)\overline{u^i u^\ell}\right]\Psi_{,i}\right)_{,\ell}$	Zero	$\gamma(P^{ij} - \frac{2}{3}P\delta^{ij})$
4	Naot et al., with wall term	$f'_\mu = 1.0$	$\epsilon^{ij} = \frac{2}{3}\epsilon\delta^{ij}$	f_ℓ	$\gamma = 0.6$
5	Launder et al., no wall term	$c_1 = 1.5$ $c_3 = 0.015$ $c_4 = 0.125$	$c_\Psi = 0.22$ $c_\epsilon = 0.15$	Zero	$-B_1(P^{ij} - \frac{2}{3}P\delta^{ij})$ $-B_2 k(U^i{}_{,j} + U^j{}_{,i})$ $-B_3(D^{ij} - \frac{2}{3}P\delta^{ij})$
6	Launder et al., with wall term		$\Psi = \overline{u^2}, \overline{v^2}, \overline{w^2}, \overline{uv}, \epsilon$ or k	f_ℓ	$B_1 = 0.764$ $B_2 = 0.182$ $B_3 = 0.109$
7	Elghobashi and Prud'homme	$c_1 = 1.17$ $c_3 = 0.123$ $c_4 = 0.003$	$\epsilon^{ij} = \frac{2}{3}\delta^{ij} + \left[\overline{u^i u^j}(\epsilon/k) f_s(1-\delta^{ij})\right]$ $f_s = 1/(1 + 1/10R_t)$	f'_ℓ	$B_1 = 0.755$ $B_2 = 0.164$ $B_3 = 0.036$

NOTE:

Common equations: k: $Dk/Dt = \text{Diff}(k) + P - \epsilon$; ϵ: $D\epsilon/Dt = \text{Diff}(\epsilon) + (\epsilon/k)(c_{1\epsilon} f_1 P - c_{2\epsilon} f_2 \epsilon) + F_\epsilon$.

Constants: $c_{1\epsilon} = 1.44$, $c_{2\epsilon} = 1.92$

$\phi_1^{ij} = c_1 \frac{\epsilon}{k}(\overline{u^i u^j} - \frac{2}{3}k\delta^{ij})$

$M = 1$: $C_\mu = 0.09$; $f_1 = f_2 = f_\mu = 1$

$M = 2$: $C_\mu = 0.09$; $f_\mu = (1 - \exp(A_\mu R_k)^2)\left(\frac{A_t}{R_t}\right)$

$f_1 = 1 + (A_{c1}/f_\mu)^3$; $f_2 = 1 - \exp(-R_t^2)$; $A_\mu = 0.0165$, $A_t = 20.5$, $A_{c1} = 0.05$

$M = 4,6$: $f_\ell = \left\{c_3\left(\frac{\epsilon}{k}\right)(\overline{u^i u^j} - \frac{2}{3}k\delta^{ij}) + c_4(P^{ij} - D^{ij})\right\}\left(\frac{k^{3/2}}{\epsilon x_n}\right)$

$M = 7$: $f'_\ell = c_3(P^{ij} - D^{ij})\exp(-c_4 R_k)$; $f'_\mu = \exp\left(-3.4\left(1 + \frac{R_t}{50}\right)^{-2}\right)$;

$F_\epsilon = c_{2\epsilon} f_\epsilon\left(\frac{\epsilon}{k}\right)\left(2\nu\sqrt{k_{,\ell}}\right) + 2\nu\left(\frac{k}{\epsilon}\right)\overline{f_\mu u_{j,m} u^{i,\ell}} U_{i,m\ell}$; $f_\epsilon = 1 - (1 - 1.41c_{2\epsilon})\exp\left(-\frac{R_t^2}{36}\right)$

Table 2 Grid selection and CPU time

Case	*Re* (000's)	Model	Grid	CPU (min)	Comments
1	10	1	120 × 40	22	
		2	120 × 66	313	54% of pts. $\leq y^+ = 40$
		3,5	120 × 50	770	High ϵ residuals
		4	120 × 50	860	
		6	120 × 40	>900	Residuals higher than for $M = 4$
		7	120 × 66	1300	See $M = 2$ and $M = 3,5$
2	38	1	120 × 50	48	
		2	120 × 66	318	30% of pts. $\leq y^+ = 40$
		3,5	120 × 50	600	
		4,6	120 × 50	658	
		7	120 × 66	>1300	30% of pts. $\leq y^+ = 40$
3,4	90	1	120 × 60	52	
	380	2	120 × 66	457	22% of pts. $\leq y^+ = 40$
		3,5	120 × 50	720	
		4,6	120 × 50	790	
					20% of pts. $\leq y^+ = 40$
		7	120 × 66	>1300	$\epsilon \rightarrow$ poor convergence
					No solution at 380,000

$M = 1$ High-*Re* k-ϵ model of Launder and Spalding[2]
$M = 2$ Low-*Re* k-ϵ model of Lam and Bremhorst[3]
$M = 3,4$ RSM of Naot et al.[7] with and without Φ_w^{ij}
$M = 5,6$ RSM of Launder et al.[6] with and without Φ_w^{ij}
$M = 7$ RSM of Elghobashi and Prud'homme[8]

where Ψ can be k, $\overline{u^2}$, $\overline{v^2}$, $\overline{w^2}$, or $\overline{uv}$. In addition, the ϵ-equation boundary condition must also be satisfied (see Ref. 1).

Presentation and Discussion of Results

Calculations were conducted for developing turbulent pipe flow at Reynolds numbers of 10,000, 38,000, 90,000, and 380,000, using an IBM 3081G computer. The estimated deviation from a grid-independent solution, determined by applying the h^m-extrapolation technique[20] to randomly selected nodal values of U and k, is estimated to be less than 5%.

Differences between results obtained using the HDS and QUICKER schemes appear mainly in the inlet region and close to the wall. These differences were small and were considered negligible for the purpose of the current investigation.

The grids used and the execution times are summarized in Table 2. The grids required when using the RSM versions are somewhat finer than those used for the associated ASM,[1] which is not surprising considering that, in the current situation, differential, as opposed to algebraic, equations are being solved. Note that when using the RSM of EP83 ($M = 7$), a solution satisfying the convergence criterion at $Re = 380,000$ could not be obtained with the grids utilized and was therefore omitted from this study.

For each of the 28 cases studied, (4 Reynolds numbers and 7 models) the values for U, V, $\overline{u^2}$, $\overline{v^2}$, $\overline{w^2}$, $\overline{uv}$, k, ϵ, τ_w, and λ have been compared to the experimental data of Richman and Azad,[21] Lawn,[22] Barbin and Jones,[23] and Nikuradse.[24] For the reasons discussed in Ref. 1, the calculations are compared to one another, and experimental data are used to place the calculations into perspective; and, even though comparisons have been made for four Reynolds numbers, the results presented here concentrate on *Re* 10,000 and 380,000 as limiting cases.

The fully developed axial mean-velocity profile is shown in Fig. 1 for $Re = 10,000$, together with experimental data.[24] The calculations are in reasonably good agreement with these data. It is noticed that a physically unrealistic change of slope (a "kink" close to the wall) in the profiles is obtained when using the RSM without the wall term ($M = 3,5$). The "sharpness" of this kink relaxes as the Reynolds number increases. It is not clear why the kink is present, although it is probably linked to the computational expediency of locating the variable $\overline{uv}$ at the grid points rather than at the corners of control volumes, see Ref. 25.

The fully developed u^+ vs y^+ profiles for three Reynolds numbers are shown in Fig. 2. The low Reynolds number k-ϵ model results are seen to be in better accord with the experimental data of Ref. 24.

In results from the high Reynolds number k-ϵ model and most RSM's ($M = 1,3$-6), τ_w is overestimated; that is, the u^+ intercept is underestimated. The sudden change in the slope for models 3 and 5 seen in this figure corresponds to the kinks observed in the axial mean-velocity profiles (Fig. 1).

The $M = 7$ case yields predictions that are not truly logarithmic in behavior; and this trend persists in a less pronounced form at higher Reynolds numbers (note that, here, poor estimation of τ_w explains the apparently large discrepancy between experimental data and predictions). A nonlogarithmic behavior suggests that the calculated turbulence field is perhaps not fully developed. Moreover, as the region described by the log-law ends at $y^+ \approx 30$, and the calculations indicate this point to be shifted to about $y^+ \approx 70$, it is argued that the RSM of EP83 exaggerates the near-wall effect. This argument will be further developed when attention is turned to the dissipation field.

The developing velocity profiles for $Re = 380,000$ are compared to those data of Ref. 23 for all models, except $M = 7$, in Fig. 3. The predictions and data are seen to be in reasonable accord. The variations of the axial velocity with distance from the inlet are shown in Fig. 4. where it is seen that excellent agreement between the predictions and the data exists, except at the centerline. Note that those data obtained by Barbin and Jones[23] at the centerline are not in agreement with those of Nikuradse,[24] although the calculations do asymptote to the values found by Nikuradse at large x/D.

The redistribution of the mean-flow momentum is effected primarily through the Reynolds shear stresses. Predictions for the $\overline{uv}$ field at $Re = 10,000$ are shown in Fig. 5 and for

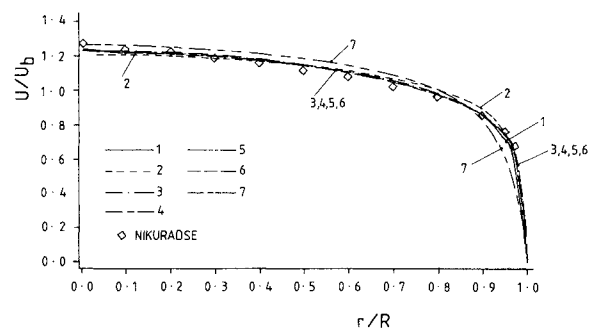

Fig. 1 Axial velocity vs r/R at $x/D = 80$ for $Re = 10,000$.

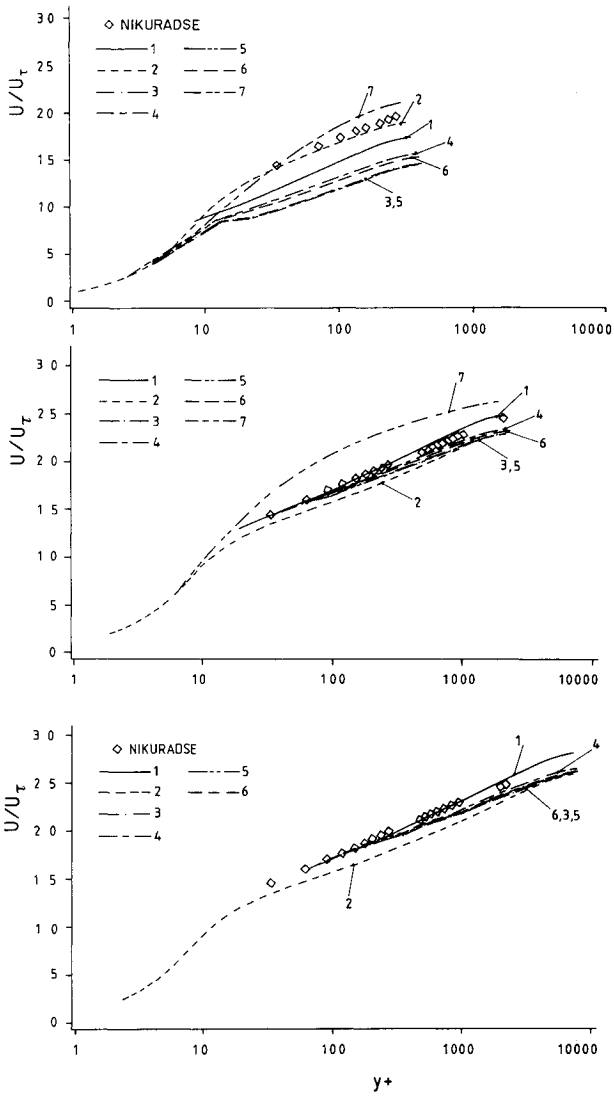

Fig. 2 u^+ vs y^+ at $x/D = 80$: a) $Re = 10{,}000$, b) $Re = 90{,}000$, c) $Re = 380{,}000$.

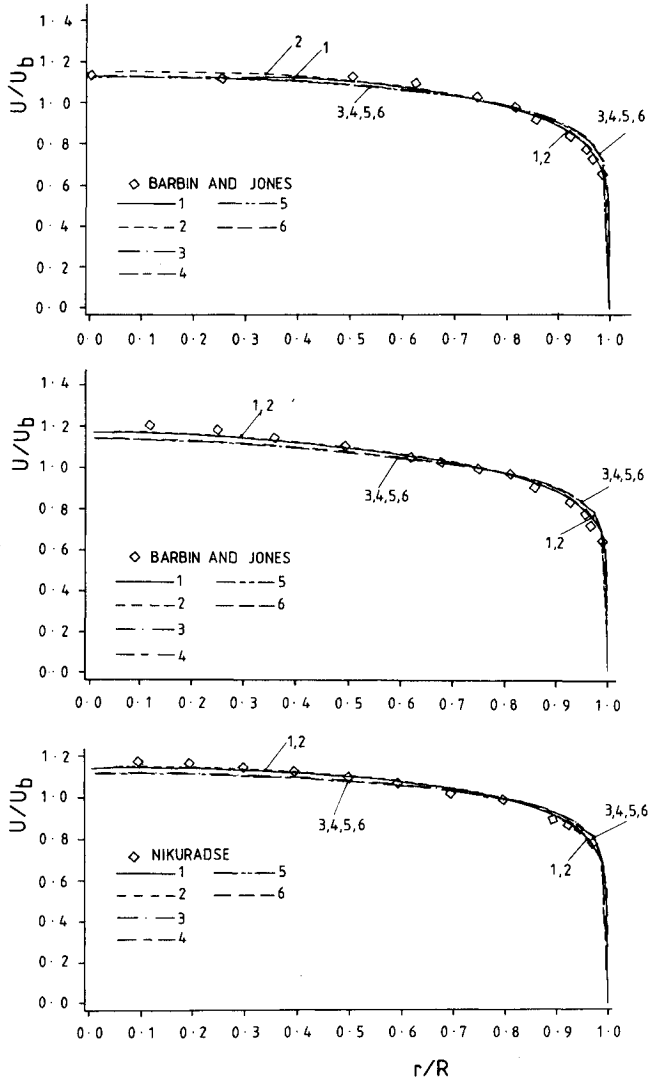

Fig. 3 Axial velocity vs r/R for $Re = 380{,}000$: a) $x/D = 16$, b) $x/D = 29$, c) $x/D = 80$.

$Re = 380{,}000$ in Fig. 6. Those data of Richman and Azad,[21] obtained at $Re = 100{,}000$, are used on the premise that the Reynolds stress profiles, when normalized by u_τ^2, show quasi-universal behavior; see Lawn.[22] From the figures, it appears that little difference exists between the predictions obtained for $\overline{uv}/u_\tau^2$; and, there seems to be only a negligible effect from the pressure-strain prescriptions in the RSM (compare $M = 3,5$ and $M = 4,6$ for Φ_2^{ij} and $M = 3,4$ and $M = 5,6$ for Φ_w^{ij}). However, at low Reynolds numbers, it is observed that the $\overline{uv}$ field as predicted by the RSM ($M = 3$–6) develops too quickly and that the wall effect is underestimated. Simulations using the RSM of EP83 and the k-ϵ models ($M = 1,2,7$) are found to be in good agreement with each other in the inlet region at low Reynolds numbers.

The effect of the wall proximity on the $\overline{uv}$ field, for the k-ϵ models, is introduced through the modeling of the length scale and the turbulence velocity scale ($k^{3/2}/\epsilon$ and $\sqrt{k}$, respectively), which are then used to describe an effective turbulence viscosity. This approach, although effective in many cases, ignores particular local physical considerations so that only global effects are simulated.

In the RSM's, the approach taken is at a more fundamental level; that is, the individual terms in the Reynolds stress transport equation are modeled. In most RSM's ($M = 3$–6), an assumption of local isotropy is made. At high Reynolds numbers, the difference between the large and small turbulence length scales is significant such that the flowfield is still well described when using local isotropy; however, at lower Reynolds numbers, the ratio between length scales is no longer large, and anisotropy becomes an important factor; for example, the dissipation term of the shear stress equations is thought to be responsible for the delay in their development at lower Reynolds numbers (see Fig. 5). EP83 used this argument to introduce an anisotropic model for ϵ^{ij}.

The magnitude of $\overline{uv}$ is greater at $x/D = 29$ than in the fully developed region (Fig. 5) for $Re = 10{,}000$ using EP83 ($M = 7$). This behavior is not unexpected, as can be seen, for example, in the results at higher Reynolds numbers for other RSM's; but the magnitude of the difference is unexpected. Because the discrepancy occurs in a region where the wall term Φ_w^{ij} is expected to have no influence and both models 6 and 7 have the same pressure-strain and production terms, these terms are discounted as possible causes for the observed behavior. It is postulated that the cause for the observed trend lies in the modeling of the turbulence diffusion term in $M = 7$.

The turbulence diffusion contribution is modeled similarly for each RSM, except that a damping function, f'_μ, is premultiplied in order to include near-wall, low Reynolds number effects. This approach is directly analogous to that in the various low Reynolds number versions of the k-ϵ models, but it is not clear that this approach is sound for the diffusion term. That is, the damping function introduced into the k-ϵ model is used to damp the shear stress field through the eddy viscosity. However, as outlined in the following, the diffusion

term is found to be damped twice.

Using the following relations, which hold in the near-wall region,

$$\frac{\partial U}{\partial r} = -\frac{1}{\kappa y}, \qquad \frac{\epsilon R}{u_\tau^3} \alpha \frac{1}{y}, \qquad u_\tau \alpha \sqrt{k}$$

the dominant portion of the diffusion term can be written as

$$\frac{1}{r}\frac{\partial}{\partial r}\left(\frac{r}{\sigma_\psi}\overline{uv}\left(\frac{k}{\epsilon}\right)\frac{\partial \psi}{\partial r}\right)$$

where σ_ψ is a constant. Now, for $M = 7$, this term has the form

$$\frac{1}{r}\frac{\partial}{\partial r}\left(c_s f'_\mu r \overline{uv}\left(\frac{k}{\epsilon}\right)\frac{\partial \psi}{\partial r}\right)$$

One can see that the diffusion term is damped twice, once explicitly through the damping function, then implicitly through the Reynolds stress. This form is, therefore, inconsistent in two ways. First, as is shown, it does not fully conform to the analogy drawn with the k-ϵ models. Second, the form of the turbulence diffusion term, which was proposed by Chou,[4] suggests that the viscous terms are additive. It is the present authors' suggestion that any modification to the turbulence diffusion term should be consistent with Chou, as his formulation remains exact under at least weak shear conditions and is at all times mathematically consistent.

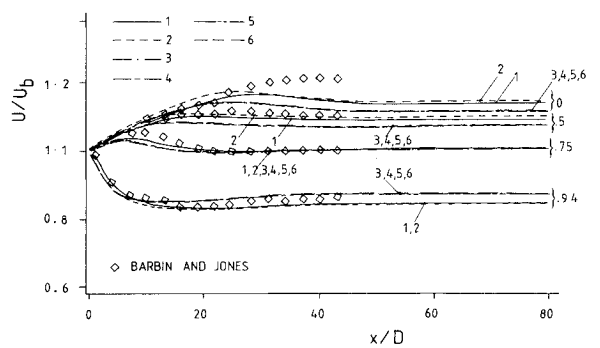

Fig. 4 Variations of axial velocity with distance downstream of pipe inlet for $Re = 380{,}000$ at $r/R = 0.$, 0.5, 0.75, 0.94.

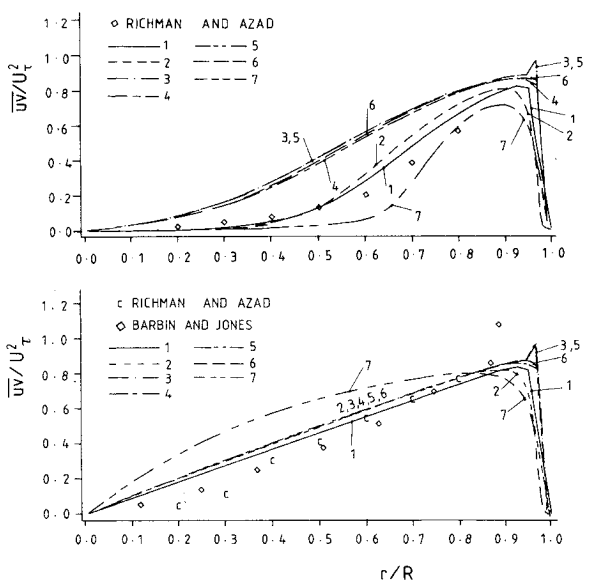

Fig. 5 Reynolds shear stress vs r/R for $Re = 10{,}000$: a) $x/D = 10$, b) $x/D = 29$.

At $Re = 380{,}000$, the predicted values for $\overline{uv}$ between $x/D \approx 25$ and $x/D \approx 40$ are greater than those in the fully developed region (see Fig. 6). However, this observation is not confirmed experimentally (e.g., Barbin and Jones[23] or Richman and Azad[21]). An adequate explanation for this phenomenon can be obtained by investigating the axial development of the mean-velocity profile (Fig. 4). Fluid is convected toward the pipe center from the inlet to the point at which the centerline velocity attains a maximum value, $x/D \approx 20$, after which the centerline velocity decreases, causing a corresponding increase in the near-wall velocity, as would be expected from the continuity equation. This process results in a negative value for both $\partial U/\partial x$ and $\partial V/\partial r$ over much of the pipe cross section between $x/D \approx 25$ and $x/D \approx 40$. The net result is an increase in the production term for $\overline{uv}$, and we may conjecture an ensuing increase in $\overline{uv}$; however, it is difficult to assess whether the production term alone is sufficiently large to account for what is predicted. It is to be noted that, at 29 and 41 diameters downstream of the pipe inlet, the value for $\overline{uv}/u_\tau^2$ can exceed those values found in fully developed flow.[23]

The radial distributions for the dissipation rate ϵ are shown in Fig. 7 for $Re = 10{,}000$, 38,000, and 380,000. The results can be discussed more conveniently by dividing the models into three groups, The first group consists of the low Reynolds number k-ϵ model and the two RSM's including the wall effect term ($M = 2,4,6$). The simulations obtained using this group

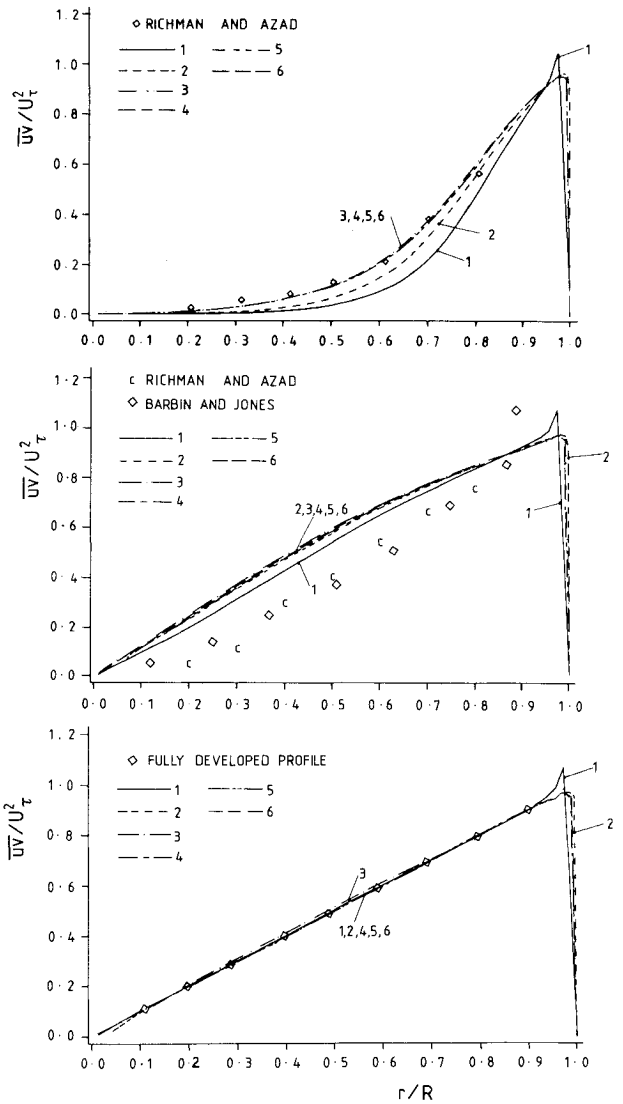

Fig. 6 Reynolds shear stress vs r/R for $Re = 380{,}000$: a) $x/D = 10$, b) $x/D = 29$, c) $x/D = 80$.

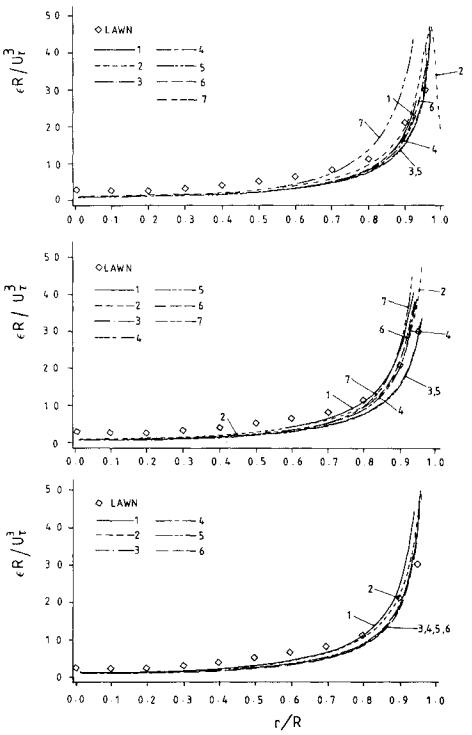

Fig. 7 Turbulence dissipation rate vs r/R at $x/D = 80$: a) $Re = 10{,}000$, b) $Re = 38{,}000$, c) $Re = 380{,}000$.

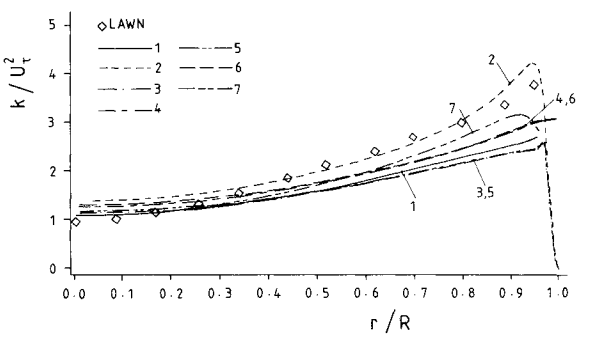

Fig. 8 Turbulence kinetic energy vs r/R at $x/D = 80$ for $Re = 10{,}000$.

display little Reynolds number dependence, in contrast to those of the second group, which consists of the high Reynolds number k-ϵ model and the RSM without wall term ($M = 1,3,5$). With reference to Lawn,[22] the results for $\epsilon R/u_\tau^3$ should depend only on $1/y$ in the fully turbulent region. The inclusion of the wall term, or a near-wall effect, reproduces this trend satisfactorily. The EP83 model constitutes the third group. The ϵ-transport equation (5) is modified to include viscous effects in the turbulence diffusion term and the wall effect term F_ϵ. As indicated previously, the suspected inconsistency in modeling the diffusion term may lead to the apparently exaggerated thickness of the near-wall region; however, it may also be suggested that the F_ϵ term plays a role in the overevaluation of the wall effect (see Fig. 8).

The radial distributions for k in the fully developed region at $Re = 10{,}000$ are shown in Fig. 8. The low Reynolds number k-ϵ model ($M = 2$) provides the best overall approximation to the experimental data. The RSM's with the Φ_w^{ij} term ($M = 4,6$) generally perform better than do the two RSM's without this term ($M = 3,5$). The EP83 model at $Re = 10{,}000$ provides a closer representation for k than the other RSM's do; but, at higher Reynolds numbers, although still maintaining a correct trend, the experimental data are not well predicted.[17]

Conclusion and Recommendations

Based on this study, the following conclusions were drawn:

1) As anticipated, the low Reynolds number k-ϵ model, which was developed for this type of flow, provides predictions that are more generally in accord with the various data sets.

2) The $\overline{u^2}$ and k fields are not well predicted by any of the RSM's in the near-wall region. It is suggested that this may be due to an unsatisfactory modeling of the diffusion and pressure-strain terms in the wall region.

3) Although not addressed here (see Martinuzzi[17]), the assumption that the flow is locally isotropic is not corroborated at low Reynolds numbers; the anisotropic effects cause the high Reynolds number models to poorly predict the shear stress field.

4) The model provided by Elghobashi and Prud'homme[8] contains many desired features, namely, anisotropic and low Reynolds number effects. However, the model, in its present form, is inconsistent in many ways and is, relative to other models, too expensive and unreliable. Note that, in this study, computer cost was not used as a criterion in model assessment.

Based on these conclusions, the authors recommend that further work of this type be considered and undertaken both experimentally and computationally in order to provide a wider and more firmly established data base for future developments. Attention should be directed particularly at establishing a canonical experiment with well-defined initial conditions, with the aims of shedding light on the behavior of the $\overline{uv}$ field in the developing flow region and of properly documenting the flowfield in the vicinity of a solid boundary.

Acknowledgments

This study was made possible by grants and graduate scholarships from the Natural Sciences and Engineering Research Council of Canada. The authors are also indebted to Queen's University for supplying unlimited computer time, without which this study could not have been undertaken. This paper was prepared while the first author was an Alexander von Humboldt Fellow at Lehrstuhl für Strömungsmechanik, Universität Erlangen-Nürnberg, Federal Republic of Germany.

References

[1]Martinuzzi, R. and Pollard, A., "A Comparative Study of Turbulence Models in Predicting Turbulent Pipe-Flow. Part I: Algebraic Stress and k-ϵ Models," *AIAA Journal,* Vol. 27, No. 1, 1989, pp. 29-36.

[2]Launder, B. E. and Spalding, D. B., "The Numerical Computation of Turbulent Flows," *Computer Methods in Applied Mechanical Engineering,* Vol. 3, 1974, pp. 269-289.

[3]Lam, C. K. G. and Bremhorst, K., "A Modified Form of the k-ϵ Model for Predicting Wall Turbulence," American Society of Mechanical Engineers, *Journal of Fluid Engineering,* Vol. 103, 1981, pp. 456-460.

[4]Chou, P. Y., "On Velocity Correlations and the Solutions for the Equations of Turbulence," *Quarterly Journal of Applied Mathematics,* Vol. 3, No. 1, 1944, pp. 38-52.

[5]Hanjalic, K. and Launder, B. E., "A Reynolds Stress Model of Turbulence and Its Application to Thin Shear Flows," *Journal of Fluid Mechanics,* Vol. 52, Pt. 4, 1972, pp. 609-638.

[6]Launder, B. E., Reece, G. J., and Rodi, W., "Progress in the Development of Reynolds-Stress Turbulence Model," *Journal of Fluid Mechanics,* Vol. 68, 1975, pp. 537-566.

[7]Naot, D., Shavit, A., and Wolfstein, M., "Interactions Between Components of the Turbulent Velocity Correlations Tensor," *Israel Journal of Technology,* Vol. 8, 1970, p. 259.

[8]Elghobashi, S. and Prud'homme, M., "Prediction of Wall Bounded Turbulent Flows with an Improved Reynolds-Stress Model," *Proceedings, IV Symposium on Turbulent Shear Flows,* Karlsruhe, 1983.

[9]Spalding, D. B., "A Novel Finite-Difference Formulation for Differential Expressions Involving Both First and Second Derivatives," *Internatonal Journal for Numerical Methods in Engineering,* Vol. 4, 1972, pp. 551-559.

[10]Pollard, A. and Siu, A. L-W., "The Calculation of Some Laminar Flows Using Various Discretization Schemes," *Computer Methods in Applied Mechanics and Engineering,* Vol. 35, 1982, pp. 293–313.
[11]Raithby, G. D. and Schneider, G. E., "Numerical Solution of Problems in Incompressible Fluid Flow: Treatment for the Pressure-Velocity Coupling," *Numerical Heat Transfer,* Vol. 2, 1979, pp. 417–440.
[12]Van Doormaal, J. P. and Raithby, G. D., "Enhancement of the SIMPLE Method for Predicting Incompressible Fluid Flows," *Numerical Heat Transfer,* Vol. 7, 1984, pp. 147–163.
[13]Harlow, F. H. and Hakayama, P. I., "Turbulence Transport Equations," *Physics of Fluids,* Vol. 10, 1967, pp. 2323–2332.
[14]Daly, B. J. and Harlow, F. H., "Transport Equations of Turbulence," *Physics of Fluids,* Vol. 13, 1970, pp. 2634–2649.
[15]Yang, C. I., Kao, T. T., Bartzis, J. G., and Sha, W. T., "Numerical Modeling of Turbulent Flow in Pipes with a Reynolds Stress Closure," ASME/ASCE Conference, Boulder, CO, 1981.
[16]Rotta, J., "Statistische Theorie Nichthomogener Turbulenz," *Zeitschrift für Physik,* Vol. 129, 1951, p. 547.
[17]Martinuzzi, R., "Comparative Study of Turbulence Models in Simulating Developing Turbulent Pipe Flow," M.Sc. Thesis, Dept. of Mechanical Engineering, Queen's Univ. at Kingston, Ontario, Canada, 1985.
[18]Champagne, F. H., Harris, V. G., and Corrsin, S., "Experiments on Nearly Homogeneous Shear Flows," *Journal of Fluid Mechanics,* Vol. 41, 1970, pp. 81–139.
[19]Patel, V. C., Rodi, W., and Scheuerer, G., "Evaluation of Turbulence Models for Near-Wall and Low-Reynolds Number Flows," *AIAA Journal,* Vol. 23, Sept. 1984, pp. 1308–1319; see also *Proceedings of Fourth Symposium on Turbulent Shear Flow,* 1983, Karlsruhe.
[20]Crandall, S. H., *Engineering Analysis,* Kruger Publishing, Malabar, FL, 1983.
[21]Richman, J. W. and Azad, R. S., "Developing Turbulent Flow in a Smooth Pipe," *Applied Scientific Research,* Vol. 28, 1973, pp. 419–441.
[22]Lawn, C. J., "Rate of Dissipation in Turbulent Pipe Flow," *Journal of Fluid Mechanics,* Vol. 48, 1971, pp. 477–505.
[23]Barbin, A. J. and Jones, J. B., "Turbulent Flow in the Inlet Region of a Smooth Pipe," *Transactions of the American Society of Mechanical Engineers, Journal of Basic Engineering,* Vol. 29, 1963, pp. 29–34.
[24]Nikuradse, J., "Gesetzmässigkeit der turbulenten Strömung in glatten Rohren," *Verein Deutscher Ingenieure-Forschungsheft,* No. 356, 1932.
[25]Huang, P. G. and Leschziner, M. A., "Stabilization of Recirculating-Flow Computations Performed with Second-Moment Closures and Third-Order Discretization," *Proceedings of Fifth Symposium on Turbulent Shear Flows,* Cornell, 1985.